# General Disclaimer

One or more of the Following Statements may affect this Document

- This document has been reproduced from the best copy furnished by the organizational source. It is being released in the interest of making available as much information as possible.

- This document may contain data, which exceeds the sheet parameters. It was furnished in this condition by the organizational source and is the best copy available.

- This document may contain tone-on-tone or color graphs, charts and/or pictures, which have been reproduced in black and white.

- This document is paginated as submitted by the original source.

- Portions of this document are not fully legible due to the historical nature of some of the material. However, it is the best reproduction available from the original submission.
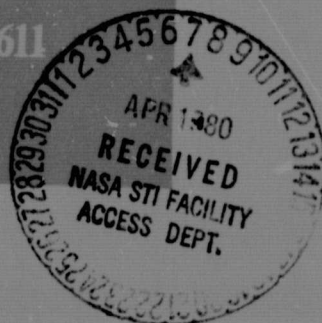
Enclosure(s)

RLF/gg

EQUAL EMPLOYMENT

FL
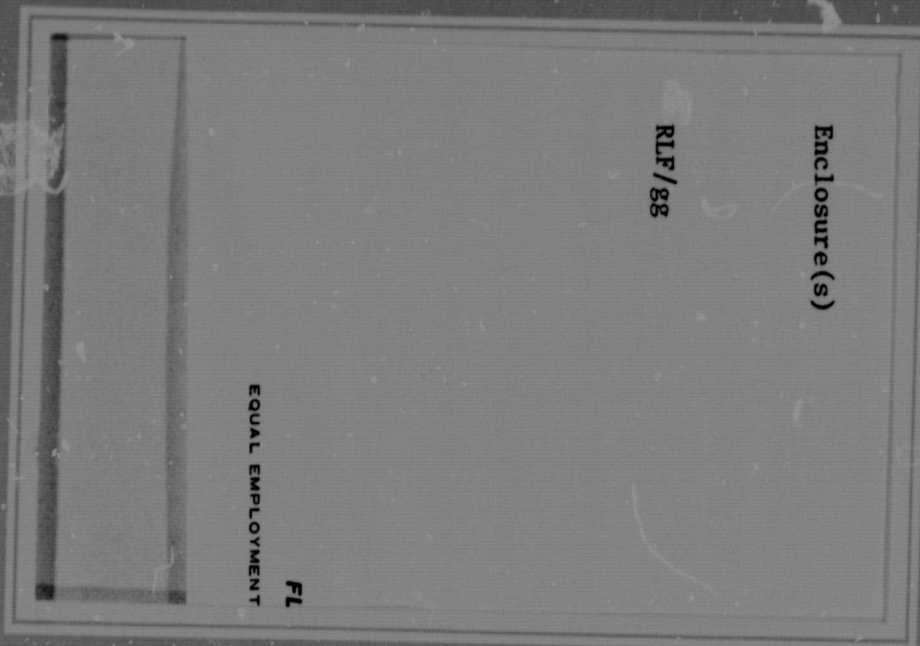
DEPARTMENT OF ENGINEERING SCIENCES

College of Engineering
University of Florida Gainesville, FL 32611

VORTICITY ASSOCIATED WITH
MULTIPLE JETS IN A CROSSFLOW

By

Susan Braden

Undergraduate

Senior Year

Engineering Sciences Department

University of Florida

Gainesville, Florida

VORTICITY ASSOCIATED WITH MULTIPLE JETS IN A CROSSFLOW

ABSTRACT

A preliminary investigation of vortex patterns from multiple subsonic jets exiting perpendicularly through a flat plate into a subsonic crossflow has been conducted at the Engineering Sciences Department, University of Florida. Two multiple jet configurations, tandem and transverse, were examined. A paddle wheel sensor was utilized to indicate the presence and relative magnitude of streamwise vorticity in the flow. This method is shown to be an effective and inexpensive way to obtain qualitative information about streamwise vorticity associated with a jet in a crossflow. Results are presented in the form of contour plots of rotational speed of the paddle wheel as measured in planes downstream from the jets and perpendicular to the crossflow. These contour plots indicate the presence of well developed diffuse contrarotating vortices for the configurations studied. The location and strength of these vortices depends on the multiple jet configuration and the distance downstream from the jets. The results for single jet cases are compared with those of previous experiments.

NOMENCLATURE

D = diameter of jet (0.404 inch)

M_j = Mach number of jet fluid at orifice

M_∞ = Mach number of cross flow fluid

R = effective velocity ratio

r_c = radius of vortex core

$r_{\frac{1}{2}}$ = distance from center of vortex to 0.5 contour

T_j = temperature of jet fluid

T_∞ = temperature of crossflow fluid

U_j = speed of jet fluid at orifice

U_∞ = speed of cross flow fluid

β = diffusion constant

ρ_j = mass density of jet fluid at orifice

ρ_∞ = mass density of cross flow fluid

ω_o = maximum vorticity of each diffuse vortex

ω = vorticity

2

INTRODUCTION

The flow field around VTOL aircraft in transition between hover and wingborn flight is complicated by jets exiting almost perpendicularly into the crossflow created by forward motion. The interference effect created by the interaction of the jet in a crossflow and the aerodynamic surface causes a loss of lift and nose-up pitching moment (ref. 1). In an attempt to understand these jet induced effects, investigators have used a simplified model in which a round jet exhausts perpendicularly through a flat plate into a subsonic crossflow. An extensive bibliography for work done prior to 1969 can be found in reference 1.

For a single jet in a crossflow, the dominant and most persistent feature of the flow field is a pair of diffuse contrarotating vortices. The presence of this vortex pair for a round jet was first detected by utilizing a paddle wheel vorticity meter in the jet plume (refs. 1 and 2). Detailed velocity measurements in the jet plume verified the presence of the vortex pair for a round jet exhausting perpendicularly through a flat plate (ref. 3). A model was developed to infer a quantitative description of the vortex pair based on selected velocity measurements (ref. 4) and it has been verified that these vortices play a prominent role in determining the pressure distribution on the aerodynamic surface through which the jet exhausts (ref. 5). A sketch of the contrarotating vortices associated with a single jet in a crossflow is shown in figure 1.

The purpose of this investigation is to utilize a paddle wheel vorticity meter to investigate qualitatively the distribution of vorticity for selected configurations of two round jets exhausting perpendicularly through a flat plate into a crossflow. The two jet configurations studied are tandem and transverse with respect to the crossflow with the two jets spaced six jet diameters apart for both configurations.

APPARATUS

The experimental investigation was conducted in the University of Florida's closed-return atmospheric wind tunnel which has an 18 in. x 30 in. open test section.

A 0.404 inch diameter jet of air was formed using a plenum chamber and a 30:1 converging nozzle. The plenum chambers were 7 in. long with a diameter of 2.1 in. Layers of honeycomb inside the chambers were used to straighten the flow. Figure 2 shows a cross section of the nozzle-plenum assembly and figures 3-5 are photographs of the tandem and transverse jet configurations in the wind tunnel test section.

Air supply for the jets was provided by clean, dry air stored externally in a 200 psi tank. The air pressure in the plenum chambers was measured using mercury manometers.

The flat plate used for the tandem configuration was a 9.9 in. by 15.9 in. by 0.25 in. aluminum plate. The holes for the jets were centered midway between the long sides of the plate. The jets were spaced 6D apart with the forward jet being 8D aft of the plate's leading edge.

The flat plate used for the transverse jet configuration was a 12.5 in. by 13.4 in. by 0.188 in. aluminum plate. The holes for the jets were located 9D aft of the leading edge with each being 3D from the plate centerline.

A paddle wheel vorticity probe was used to locate and measure the relative strengths of the vortices. The probe consisted of four unpitched blades (see fig. 6) connected to a shaft which spins on jewelled bearings. The probe was held by a traversing mechanism located above the tunnel which moved the probe in the y and z directions (see figs. 7 and 8) with an accuracy of ± 0.03 in. The probe produced an electronic signal which was coupled to electronic equipment consisting of a counter, a digital

4

readout, and a printer that recorded the data. The design of the probe and electronics limited accuracy in situations of weak vorticity. The probe could be used to locate these areas of low vorticity, but not to accurately measure their strength.

TEST PROCEDURES AND CONDITIONS

The basic parameter used in determining test conditions for jet in a crossflow experiments has been the ratio of momentum flux across the jet exit plane to the momentum flux of the crossflow through an equal area. The effective velocity ratio is defined as the square root of the momentum ratio.

$$R = \left[\frac{\int_A \rho_j U_j^2 \, dA}{\rho_\infty U_\infty^2 A_j} \right]^{\frac{1}{2}}$$

If $T_j = T_\infty$, and U_j is constant over the entire jet orifice, then the effective velocity ratio becomes $R = M_j/M_\infty$. For incompressible flow, this reduces to U_j/U_∞ (ref. 3). For the tandem configuration, effective velocity ratios of 4 and 8 were utilized. Only R=8 was used for the transverse configuration.

Prior to the wind tunnel experiments, the characteristics of the jet nozzles exhausting into still air were examined. The jet exit plane velocity profile was found to be flat to within ± 0.1% over 98% of the jet opening.

The jet Mach number was determined by measuring the pressure in the plenum and assuming isentropic flow. For a jet to crossflow velocity ratio of 8, a crossflow Mach number of 0.09 and a jet Mach number of 0.72 were utilized. For a ratio of 4, a crossflow Mach number of 0.11 was used with a jet Mach number of 0.44. These conditions were determined by the upper crossflow limit for R=4 and by a reasonable duration of airflow from the jet nozzle for the R=8 condition. Normal variations in temperature were not taken into consideration as they would not measurably

5

alter the vortex pattern (ref. 4).

The y-z traversing mechanism was used to form a grid of measurements with 0.125 inch spacing in the y direction and 0.25 inch spacing in the z direction. The vorticity at each y-z location was measured in counts per second during ten intervals, each of one second duration, and recorded by the printer.

Vorticity measurements were made with the vorticity probe in a plane perpendicular to the crossflow located 13.00D behind the forward jet in the tandem configuration. For the transverse configuration, measurements were made in planes 13.00D and 8.66D behind both jets (see figs. 7 & 8). At each cross-section the vorticity probe was aligned tangent to the vortex curve (fig. 1) (ref. 4).

RESULTS AND DISCUSSION

Results are presented in the form of contour plots of rotational speed of the paddle wheel which is a direct indication of vortex strength. The actual values used in plotting the contours are normalized arithmetic averages of the ten measurements taken at each y-z location. For the tandem configurations, the normalization value is the average of the maximum values of both vortices in the forward jet only condition. In the case of R=8, the normalization value is 174.8 counts per second and, for R=4, it is 57.25 CPS. For the transverse configuration, the values are normalized by the average of the maximum values of each vortex in both single jet conditions. The normalization values are 230.7 and 152.1 counts per second for X/D=8.66 and X/D=13.00, respectively.

The lines shown on the plots are percentages of these normalization values. The plots are arranged in groups of three so that the relative strengths and positions of the vortex pairs associated with single and

6

multiple jets may be compared for each of the configurations (figs. 9-12).

The geometry of the single jet cases compares favorably to the results of previous experiments which involved more accurate and extensive measurements than this study (fig. 13-14).

The radius of the vortex core, r_c, has been defined as the distance from the center of a single Gaussian distribution of vorticity to the radius at which the maximum tangential speed occurs (ref. 4). The Gaussian distribution of vorticity can be represented by

$$\omega(r) = \omega_o e^{-\beta^2 r^2}$$

where β is a diffusion constant and ω_o is the maximum vorticity of the diffuse vortex. Using this relationship, the distance to the 0.5 contour of vorticity is found to be

$$r_{\frac{1}{2}} = \frac{0.693}{\beta}$$

Knowing that

$$r_c = \frac{1.121}{\beta}$$

(ref. 4) a relationship can be found between $r_{\frac{1}{2}}$ and r_c.

$$r_c = 1.35 \, r_{\frac{1}{2}}$$

The values for $r_{\frac{1}{2}}$ can be estimated for each vortex from the contour plots of vorticity (figs. 9-12) and r_c easily computed. The values for r_c/D for the single jet cases compare favorably to previous work (fig. 15).

The flux of vorticity of a single Gaussian distribution of vorticity through a surface bounded by a curve of radius R can be expressed as

$$\Gamma_{(R)} = \int_0^{2\pi} \int_0^R \omega_o e^{-\beta^2 r^2} r \, dr \, d\theta = \frac{\pi \omega_o}{\beta^2} (1 - e^{-\beta^2 R^2})$$

7

Note that when $R=\infty$, $\Gamma = \dfrac{\pi \omega_0}{\beta^2}$; substituting this into the equation for $\Gamma(R)$ and putting $e^{-\beta^2 r^2}$ in terms of ω and ω_0,

$$\Gamma_{(R)} = \Gamma_\omega (1 - \frac{\omega(R)}{\omega_0})$$

From this, a relationship can be found between the strength inside the 0.5 contour and the total strength of the vortex.

$$2\Gamma(r_{\frac{1}{2}}) = \Gamma_\infty$$

Since low levels of vorticity could not be measured with the probe, the above relationship could be used to calculate the strength of a single Gaussian vortex from the vorticity distribution for $R \leq r_{\frac{1}{2}}$. The values for $\Gamma(r_{\frac{1}{2}})$ were calculated by assuming

$$\Gamma = \frac{2\pi \Delta A}{C} \sum_{i=1}^{M} \sum_{i=1}^{N} K_{ij}$$

where ΔA is an increment of grid area, K is the number of counts per second, and C is a probe calibration constant. For a perfect probe, C equals 1. The values for Γ_R for the single jet cases were non-dimensionalized by $2U_\infty D$ and compared to values from previous tests. From this comparison a probe calibration constant of 0.45 was determined. The values plotted in figure 16 have been corrected by this constant. The dimensionless value for Γ is denoted by γ.

The tandem jet plots with both jets on (figs. 9C and 10C) indicate that the individual vortex pairs do not maintain their original identities, but rather tend to coalesce into one large pair of vortices. The new vortex pair formed is somewhat higher than for the forward jet only, and, in the case of R=8, the pair is also elongated in the vertical direction (fig. 10C). One possible explanation is that the after jet, being in the wake of the forward jet, is relatively untouched

8

by the crossflow and travels nearly straight up until it impinges on the underside of the forward plume. A constructive interference may be visualized at this point, the result being the elongated and raised vortex pattern. The R=4 pattern (fig. 9C) displays a somewhat less pronounced version of the R=8 plot due to the lower jet velocities. The geometry, vortex core size, and strength are compared with the single jet cases in figs. 13-16.

The plot of the transverse configuration at $\frac{X}{D}$ = 13.00 with both jets on indicates only the outer vortex from each jet was present (fig. 11C). A large area of low vortex strength was seen to occur in the area where one might expect to find the inner vortices. Due to design limitations of the vortex probe and associated electronics, the vortex strength in this area could not be measured accurately and is instead represented by a stippled region existing in and around the vortex peaks. This might suggest that a destructive interference between the two inner vortices has occurred.

Based on the results shown in fig. 11C, it was decided to examine a cross-section nearer to the jets.

The plot of the transverse jets with both jets on at $\frac{X}{D}$ = 8.66 shows that the inner vortices are present, but they are significantly weaker than the outer vortices and centered nearer to the plate (fig. 12C).

Potential flow calculations of the velocity induced at each vortex by the other three vortices indicate that the outer vortices should have a greater Z component of velocity than the inner vortices (fig. 17). The magnitude of this difference is a function of the vortex spacing and strength. In the case of a single pair of contrarotating vortices, both have the same drift velocity.

9

CONCLUDING REMARKS

The paddle wheel vorticity probe has been found to be a simple and inexpensive method to qualitatively examine the vorticity associated with jets in a crossflow. The geometry can be determined with a high degree of certainty, and the strength and vortex core can be reasonably approximated.

The patterns of vorticity associated with the multiple jet cases seem to be simple enough to develop a model similar to that for the single jet cases to determine a quantitative description of the vorticity. From this model, the pressure distribution on the aerodynamic surface could be predicted.

REFERENCES

1. Margason, R. J. and Fearn, R. L.: Jet-Wake Characteristics and their Induced Aerodynamic Effects on V/STOL Aircraft in Transition Flight. NASA SP-218, 1969.

2. Powell, G.: An Experimental Study of a Jet in a Subsonic Cross-Flow. Senior Research Paper, University of Florida, Dec. 1972.

3. Fearn, R. L. and Weston, R. P.: Induced Velocity Field of a Jet in a Crossflow. NASA TP-1087, 1978.

4. Fearn, R. L. and Weston, R. P.: Vorticity Associated with a Jet in a Crossflow. AIAA Journal, Vol. 12, No. 12, Dec. 1974.

5. Dietz, W. E. Jr.: A Method for Calculating the Induced Pressure Distribution Associated with a Jet in a Crossflow. M. S. Thesis, University of Florida, 1975.

6. Fearn, R. L. and Weston, R. P.: Velocity field of a Round Jet in a Crossflow for Various Jet Injection Angles and Velocity Ratios. NASA TP-1506, 1979.

ACKNOWLEDGEMENTS

The author would like to thank her advisor, Dr. Richard L. Fearn, for the opportunity to work on this project. His guidance and support have been instrumental in its successful completion.

12
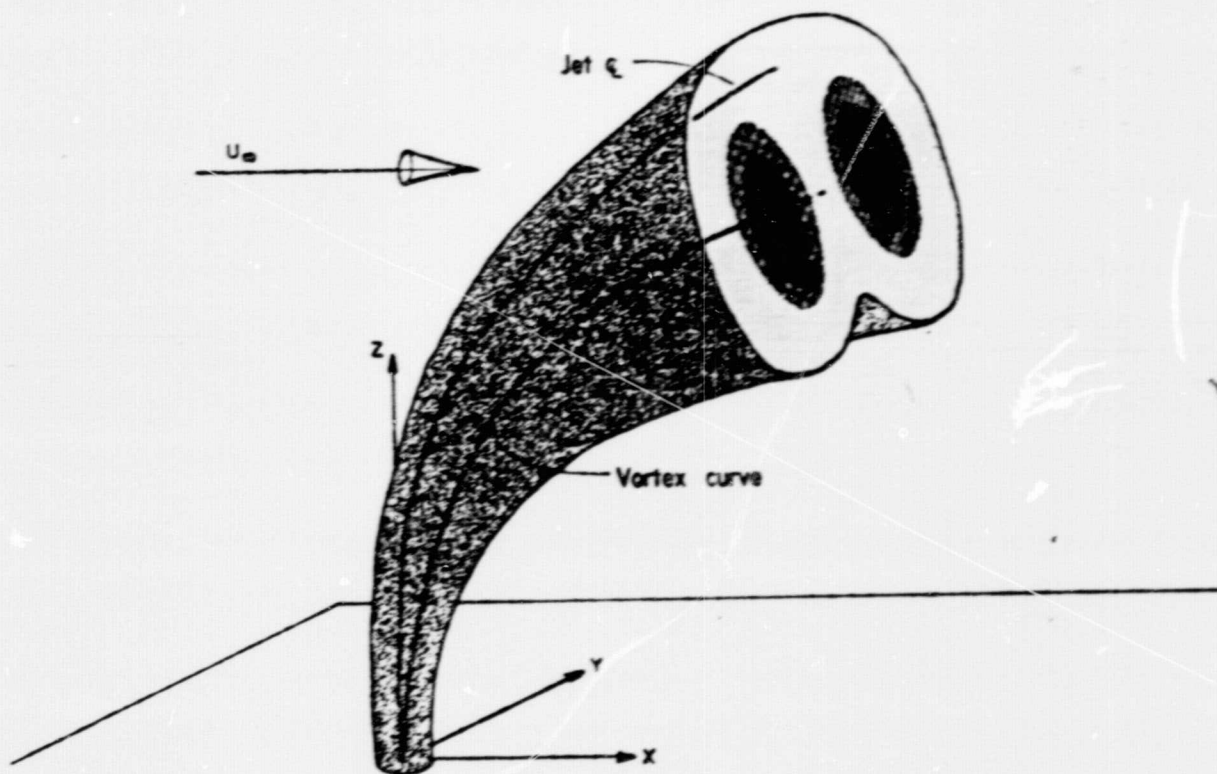
Fig.1   Sketch of a jet in a crossflow.

13
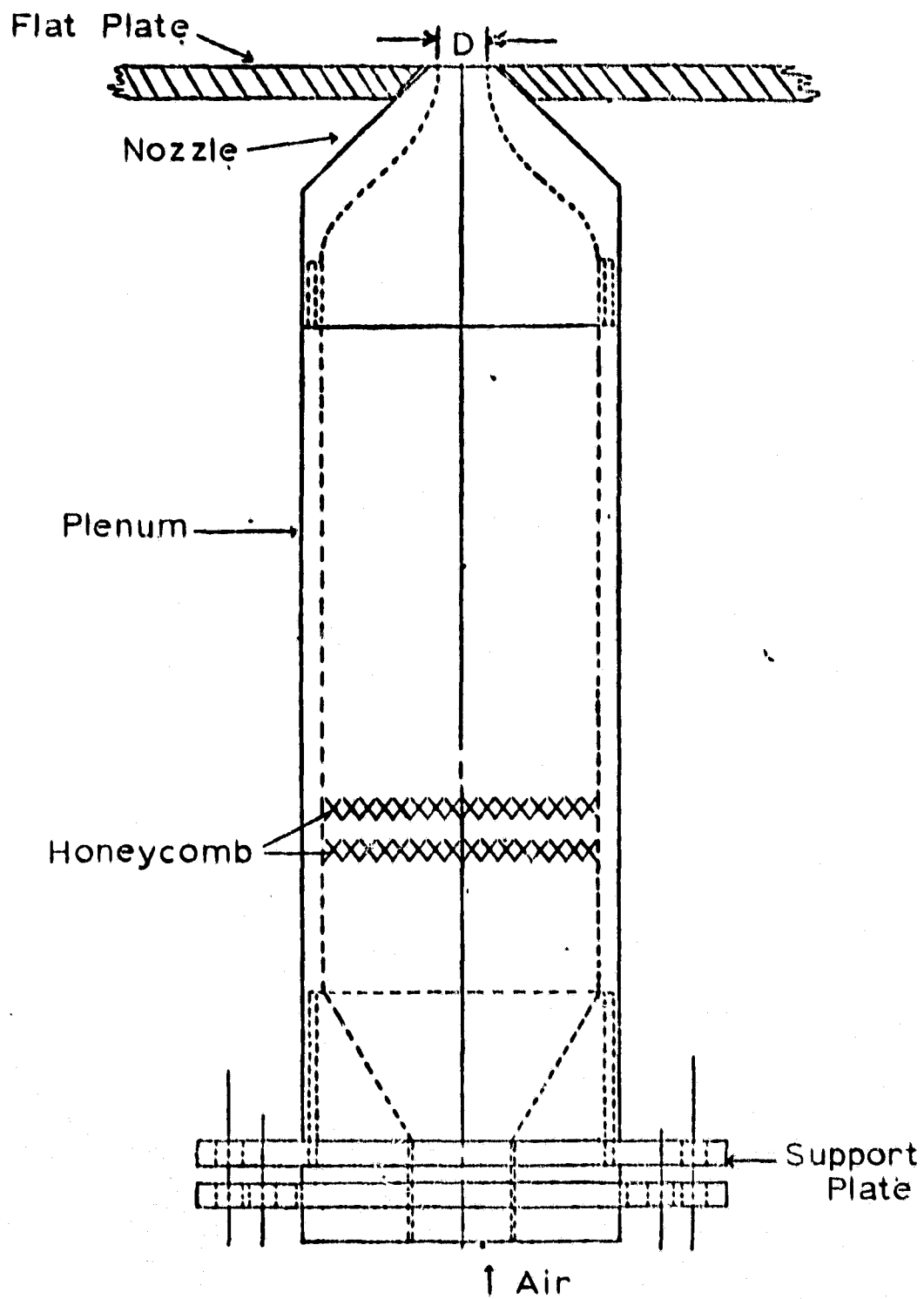
Figure 2. Nozzle - plenum assembly.
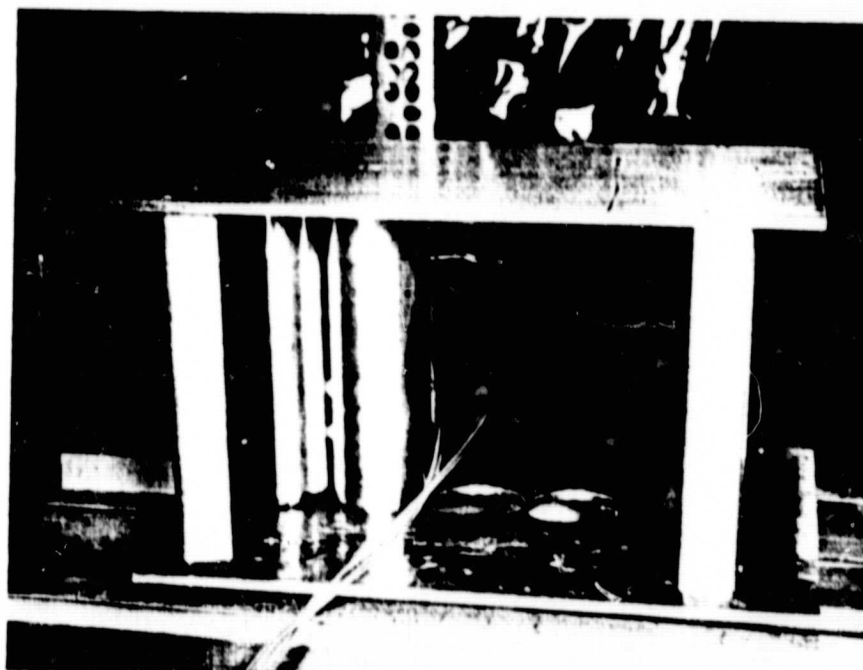
Figure 3. Tandem jet configuration.
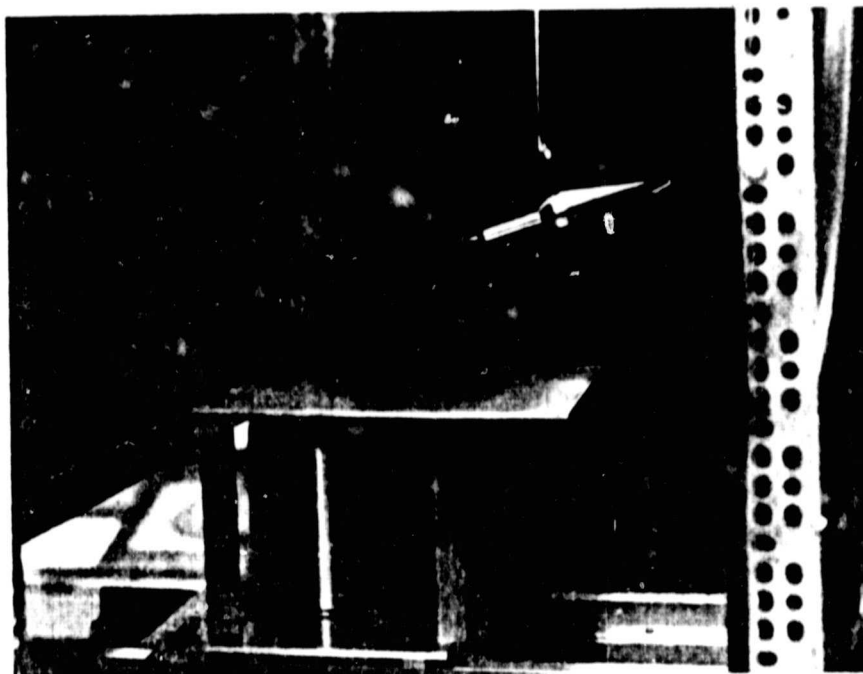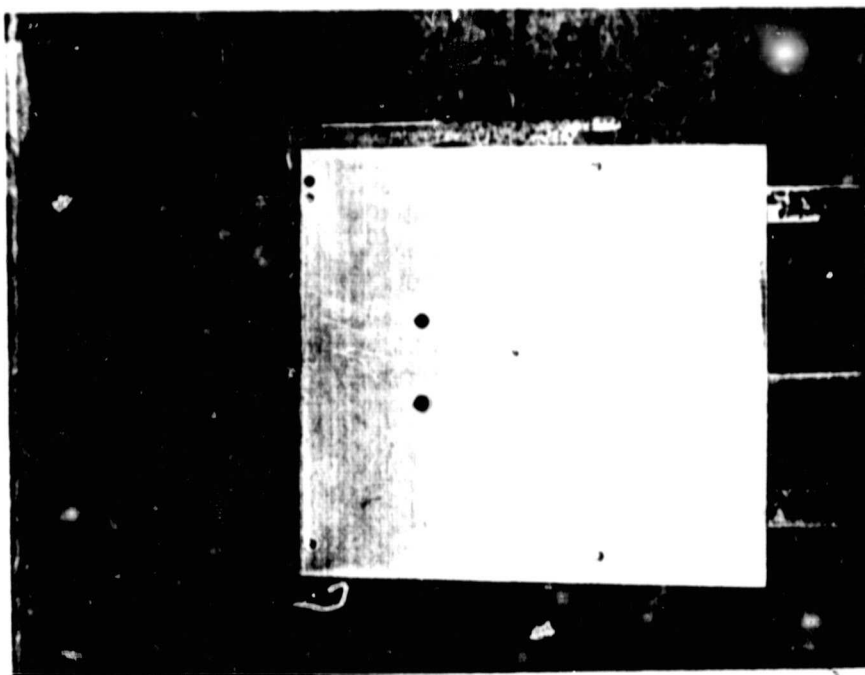
Figure 4. Transverse jet configuration.
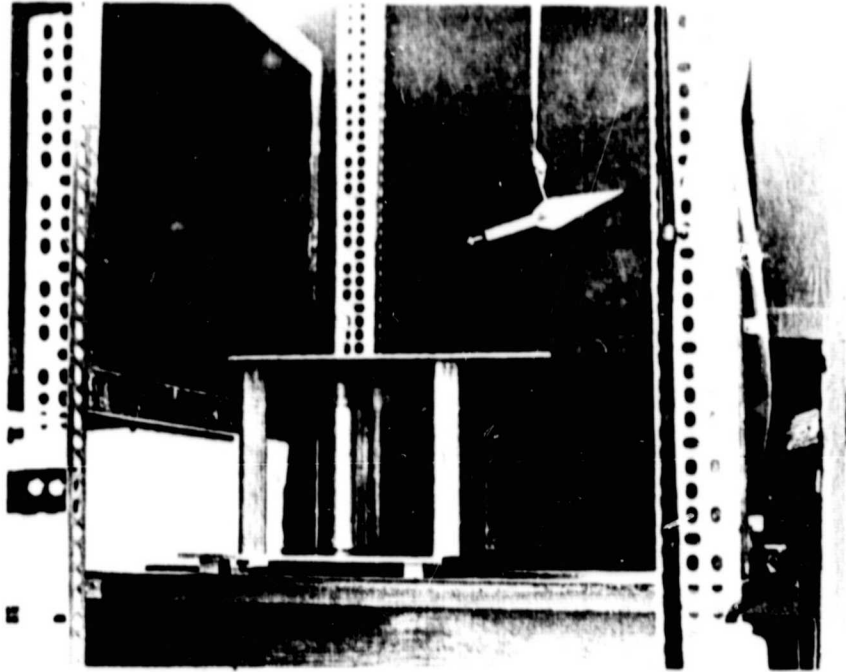
Figure 5. Apparatus in wind tunnel.
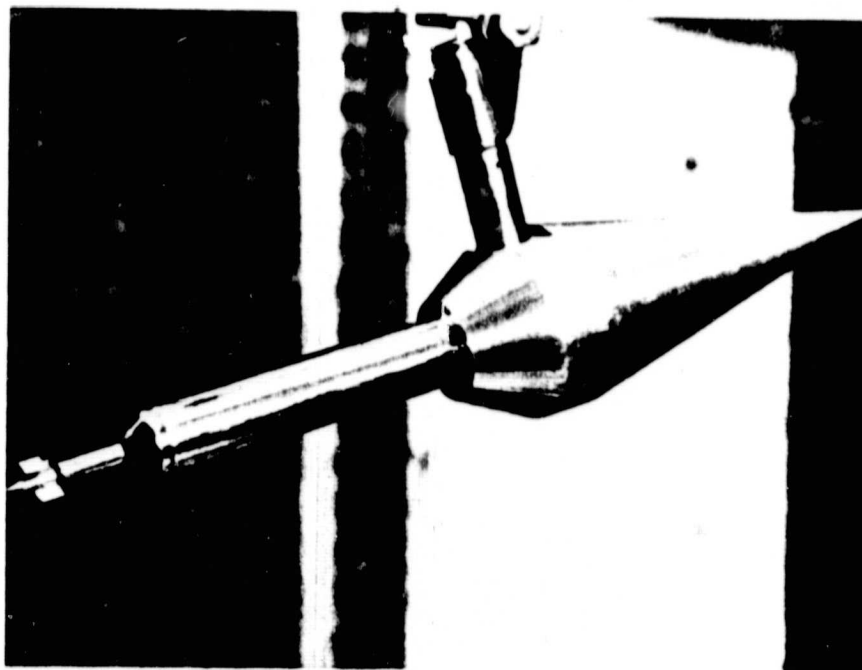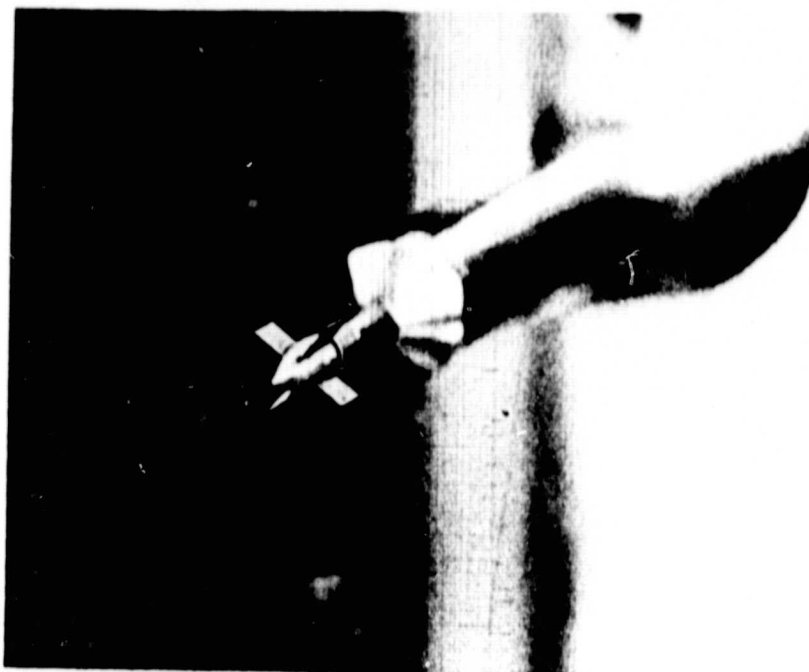
Figure 6. Vorticity probe.
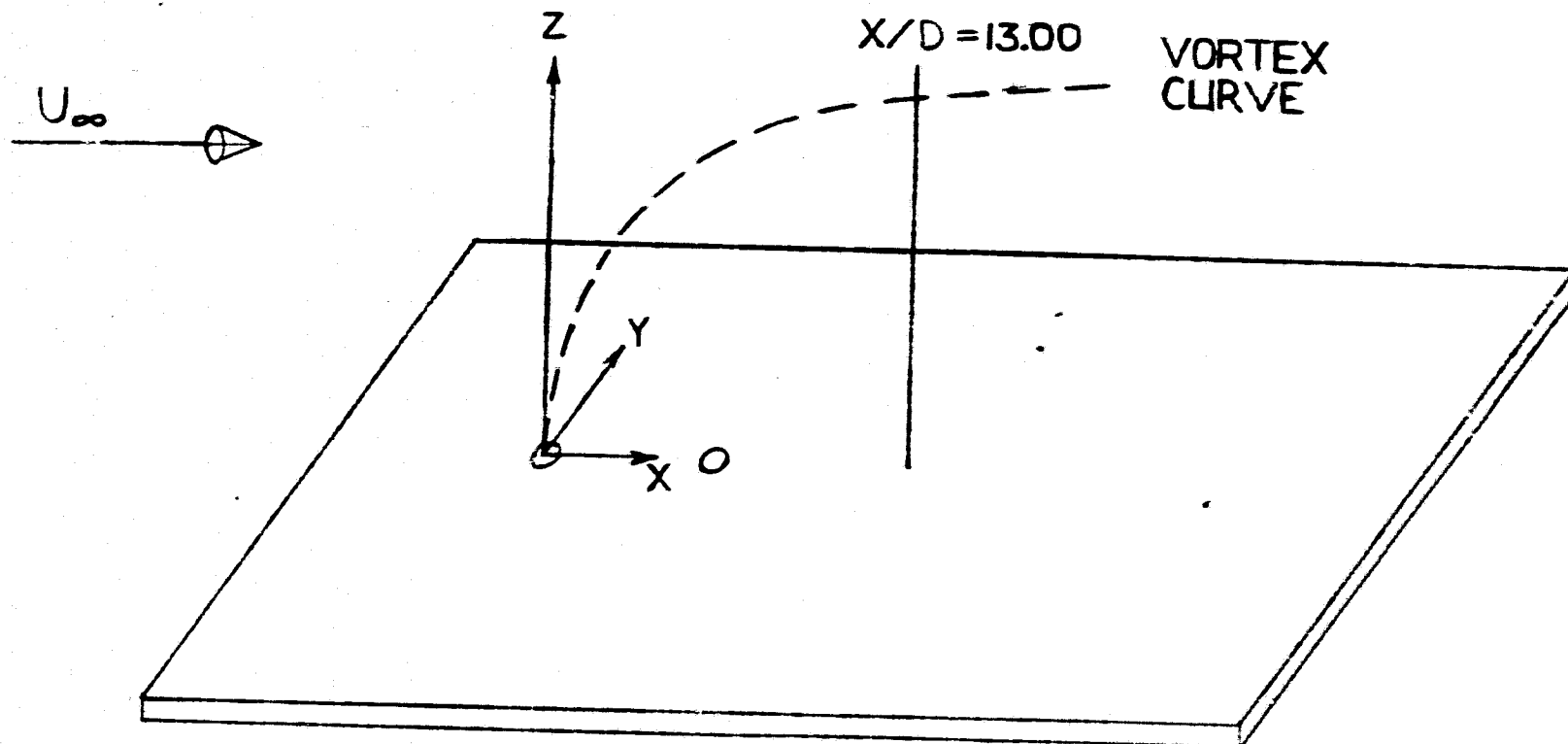
Figure 7.   Tandem jet configuration.
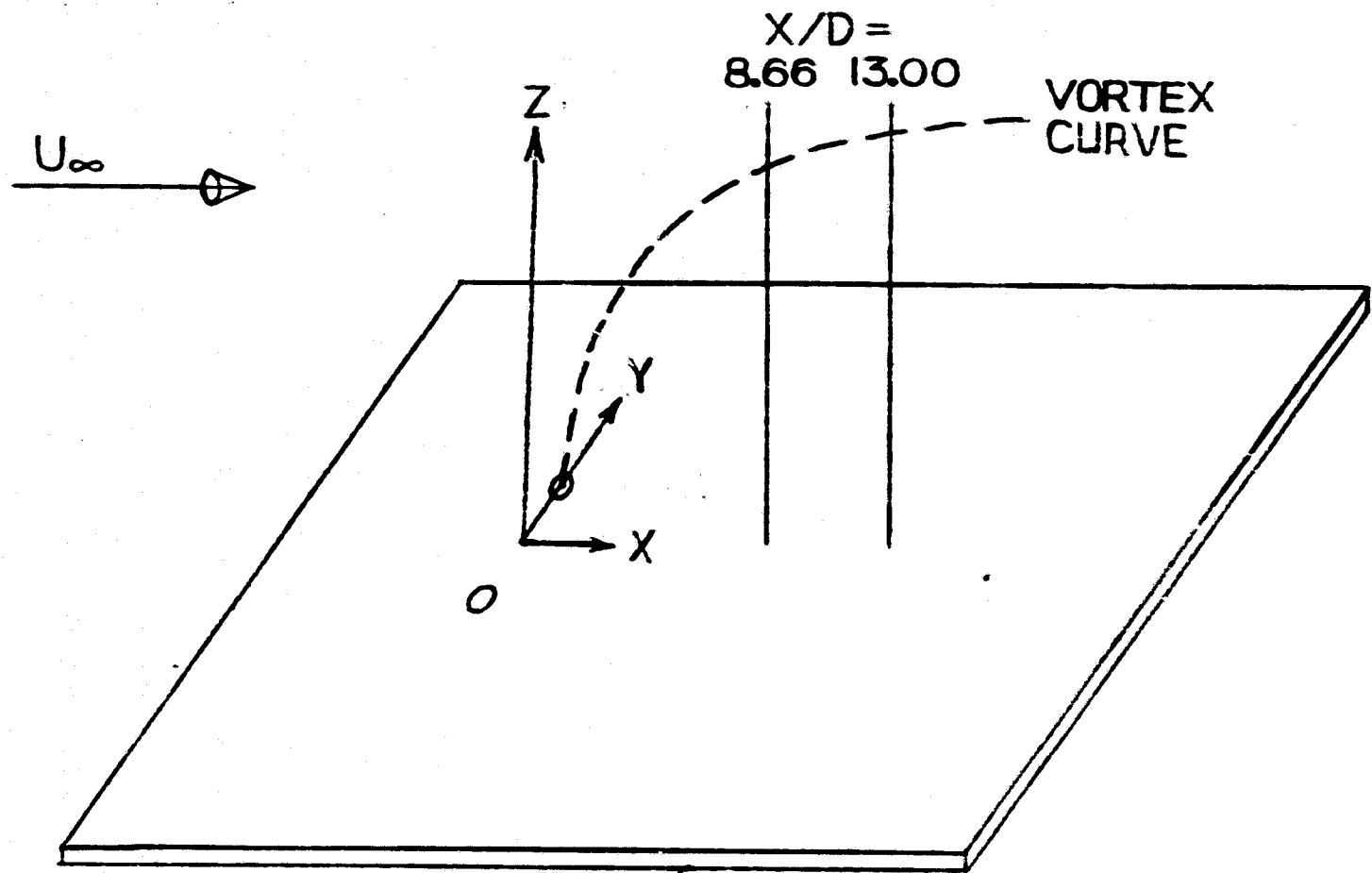
Figure 8.   Tranverse jet configuration.
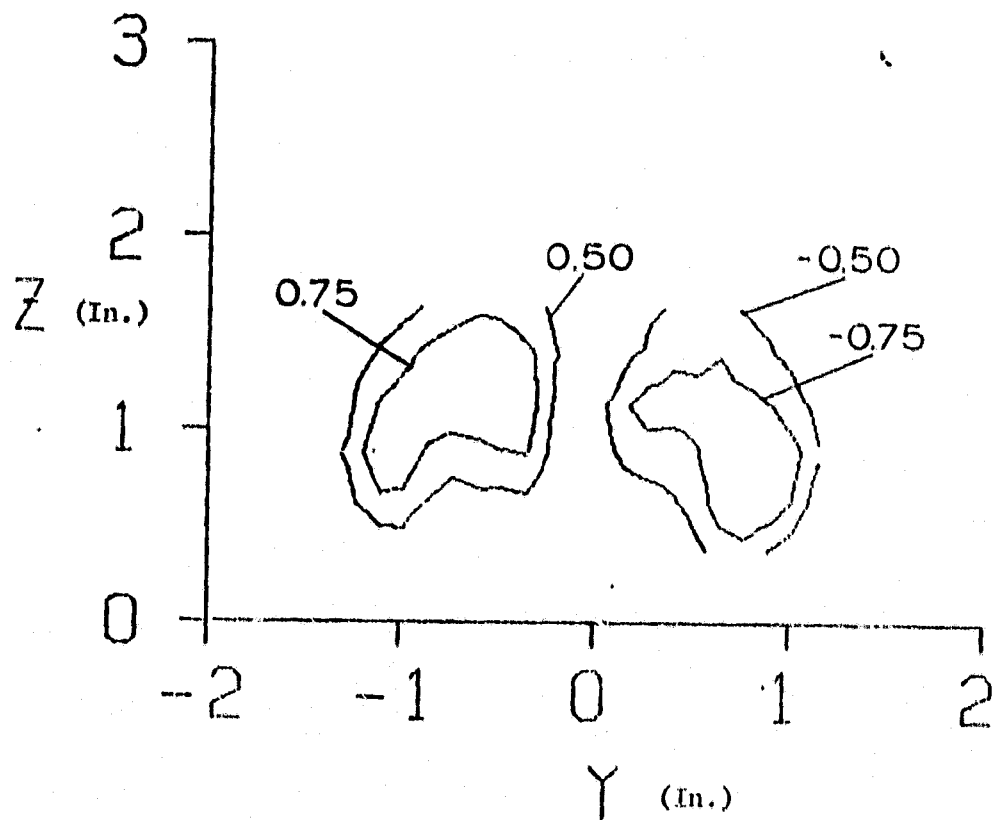
R=4, X/D=13.00

(a) Front jet only.
Figure 9. Tandem jets.

21
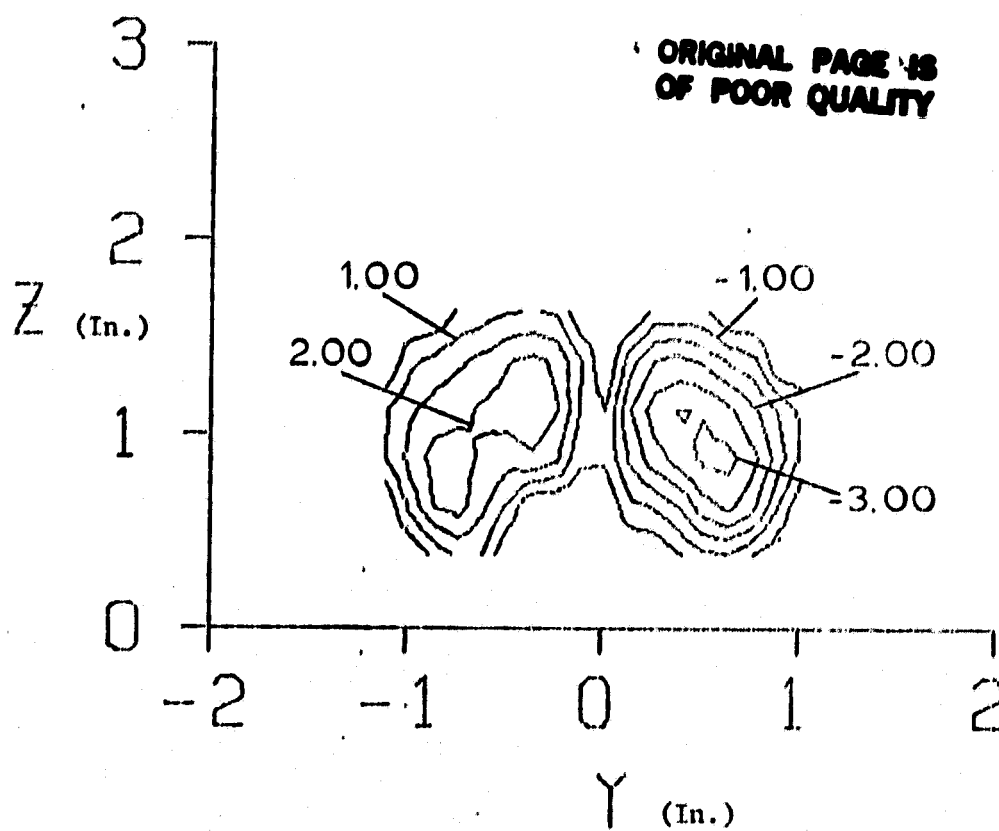
R=4, X/D=7.00.

(b) Rear jet only.
Figure 9. Continued.
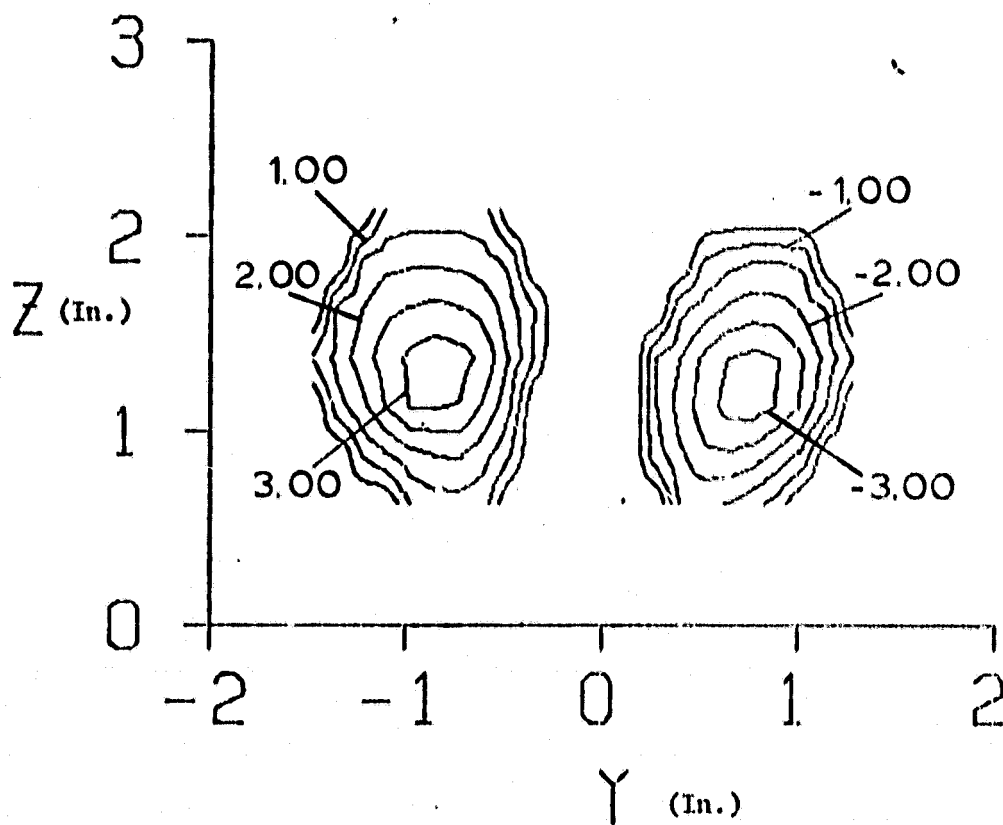
R=4, X/D=13.00
(c) Both jets.
Figure 9. Continued.

23
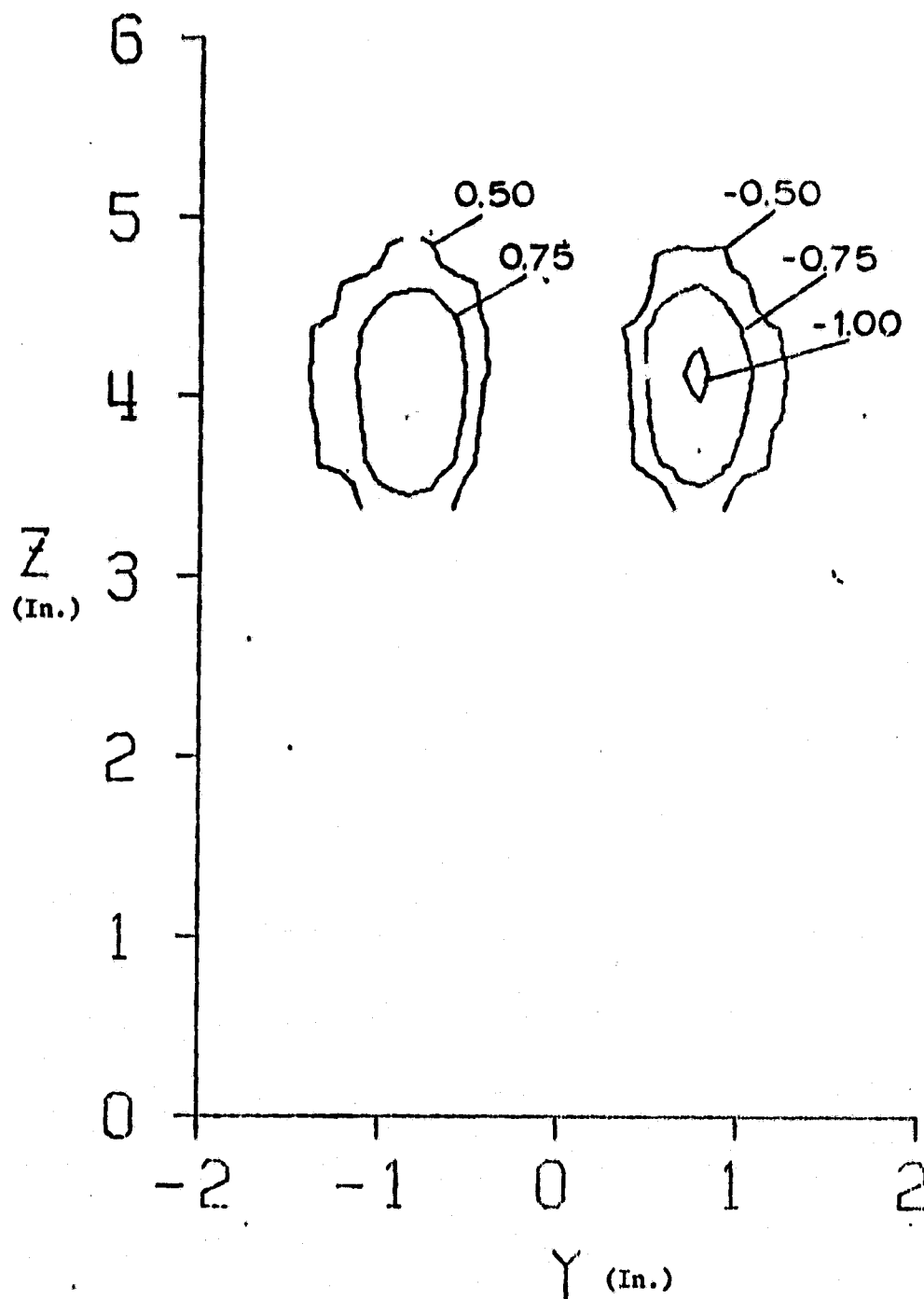
R=8. X/D=13.00.
(a) Front jet only.
Figure 10. Tandem jets.
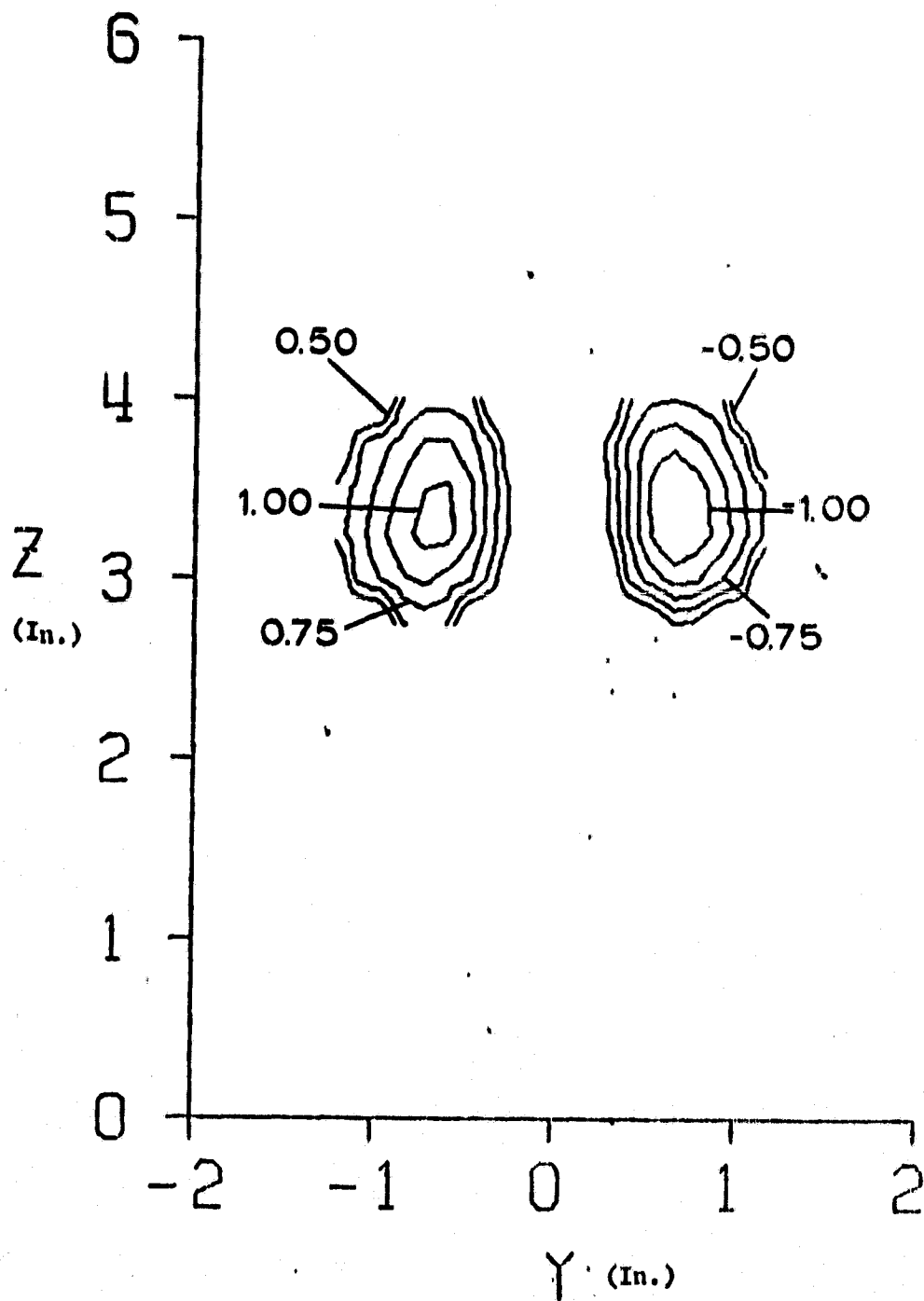
R=8.   X/D=7.00

(b) Rear jet only.
Figure 10.   Continued.

25
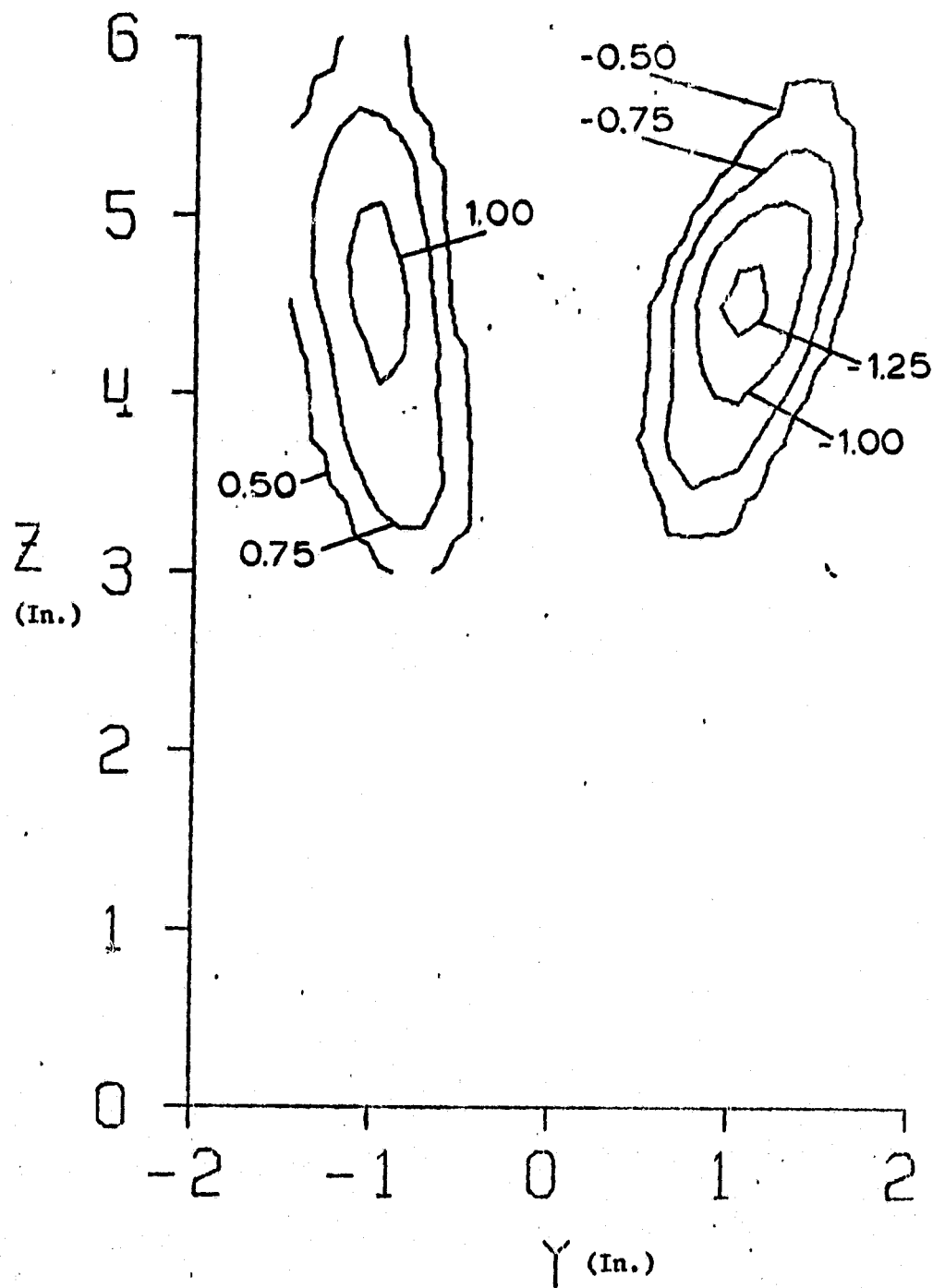
R=8. X/D=13.00.
(c) Both jets.
Figure 10. Continued.

26
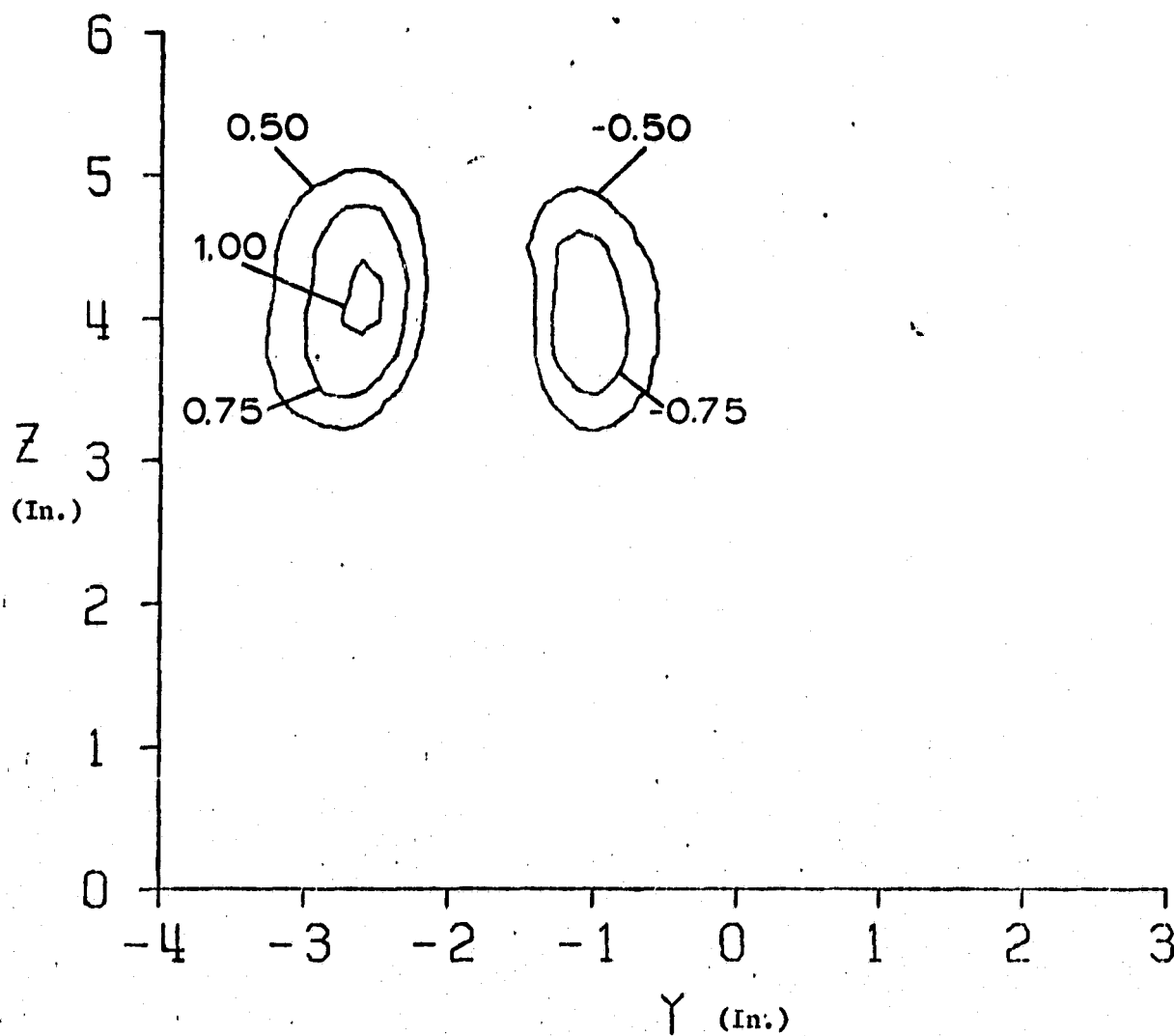
R=8. X/D=13.00

(a) Left jet only.
Figure 11 Transverse jets.
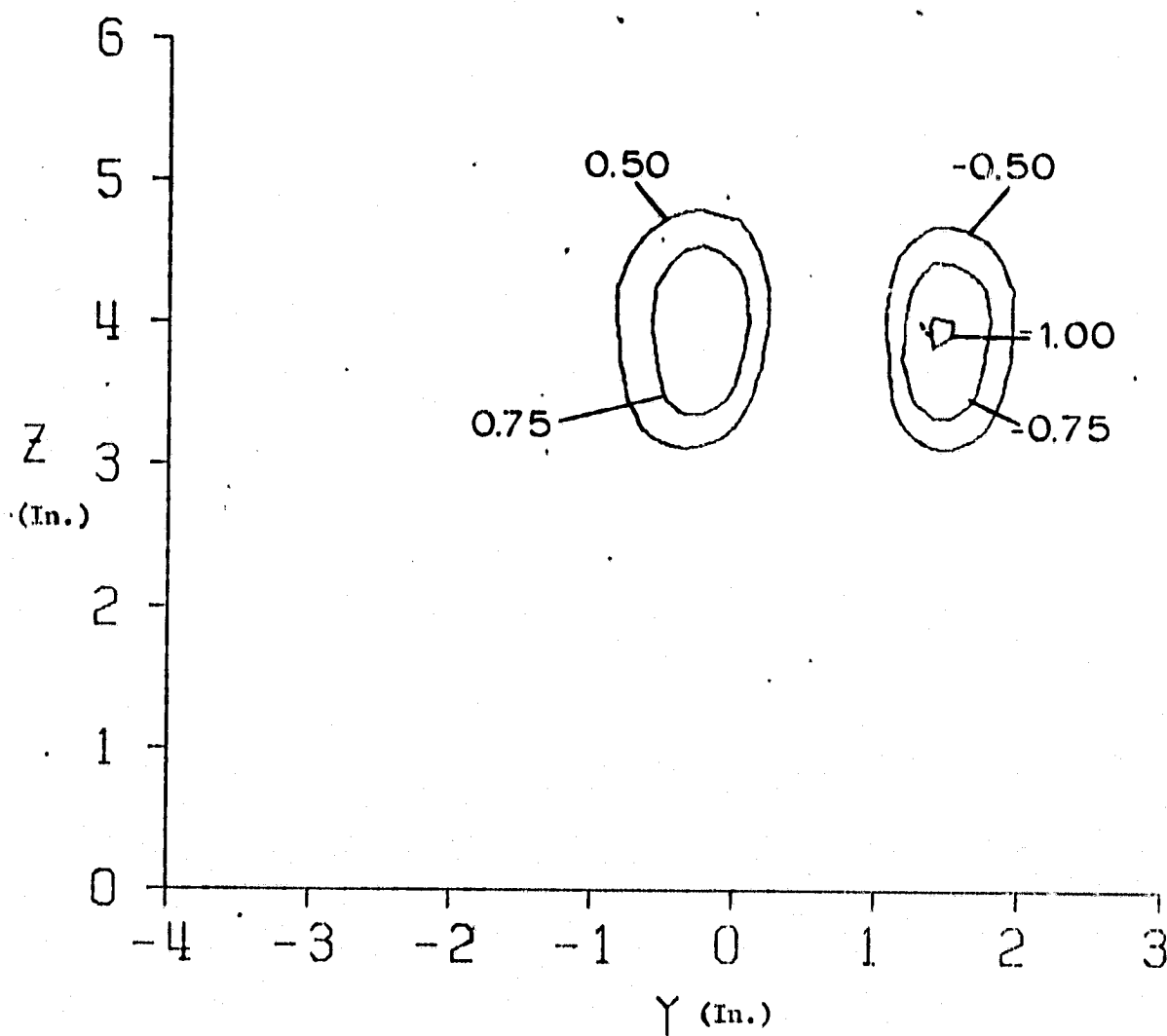
R=8.   X/D=13.00

(b) Right jet only.
Figure 11.   Continued.
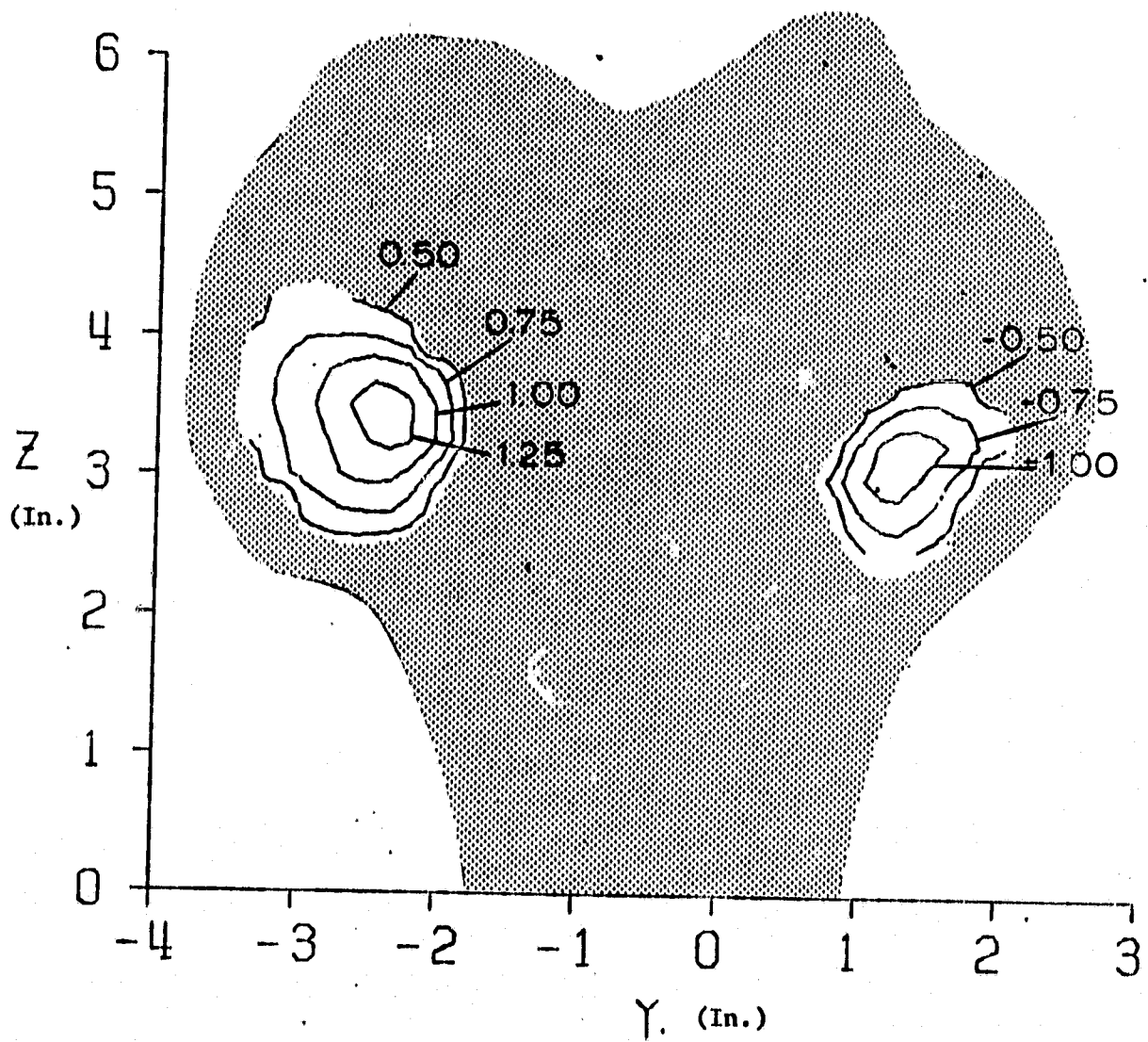
R=8.   X/D=13.00.

(c) Both jets.

Figure 11   Continued.
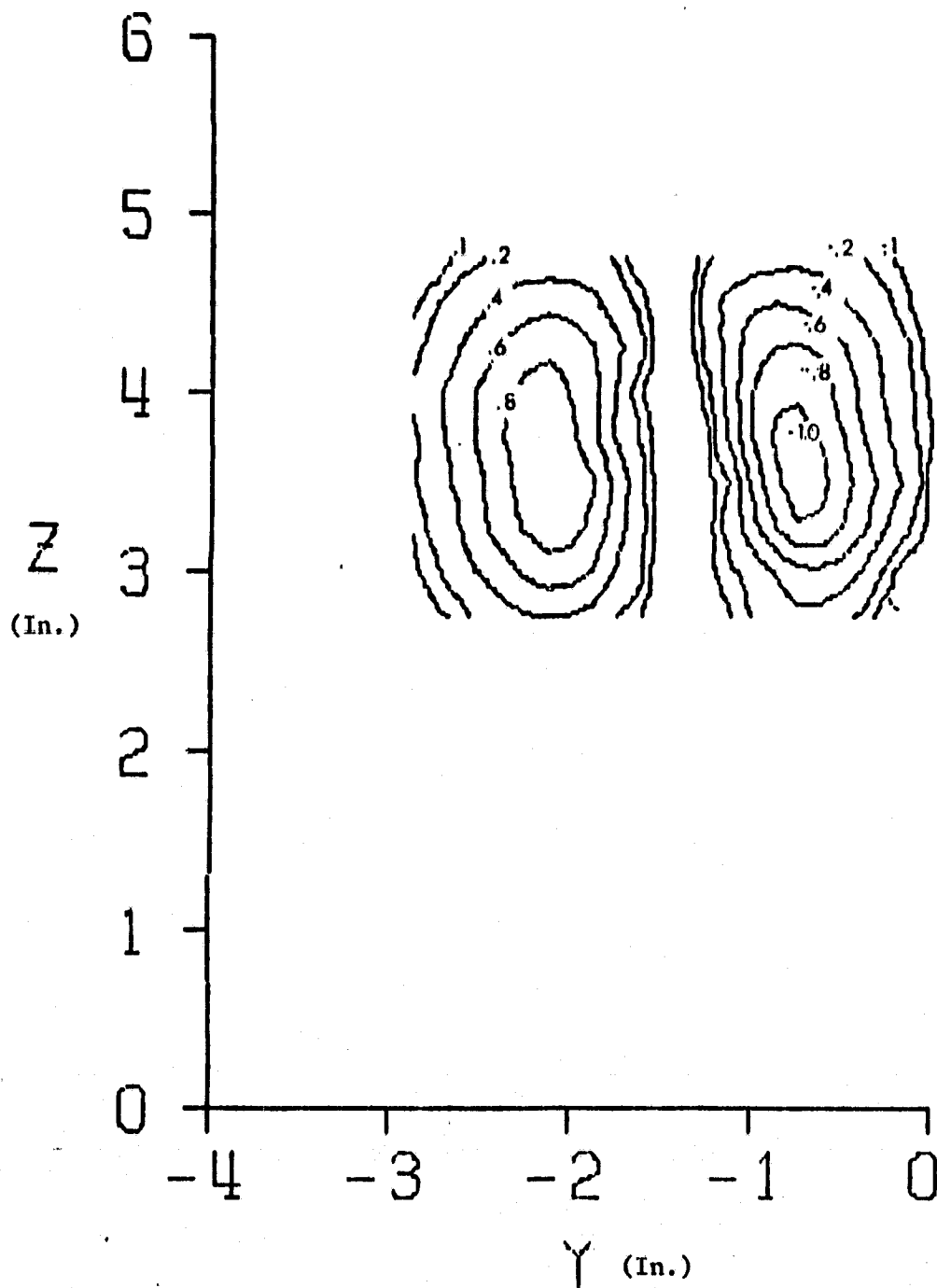
R=8.   X/D=8.66.

(a) Left jet only.
Figure 12.   Transverse jets.
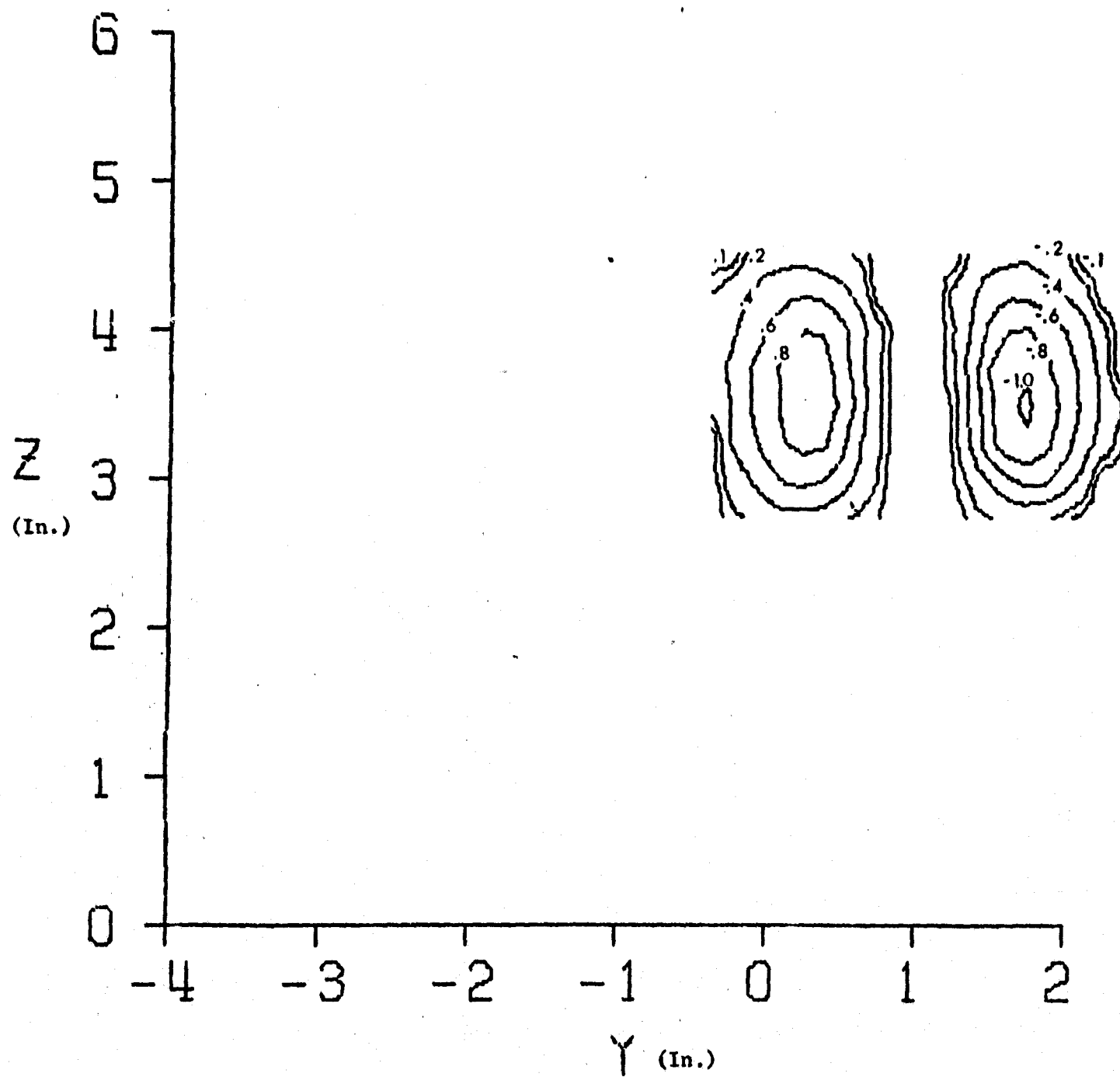
R=8. X/D=8.66.

(b) Right jet only.

Figure 12. Continued.
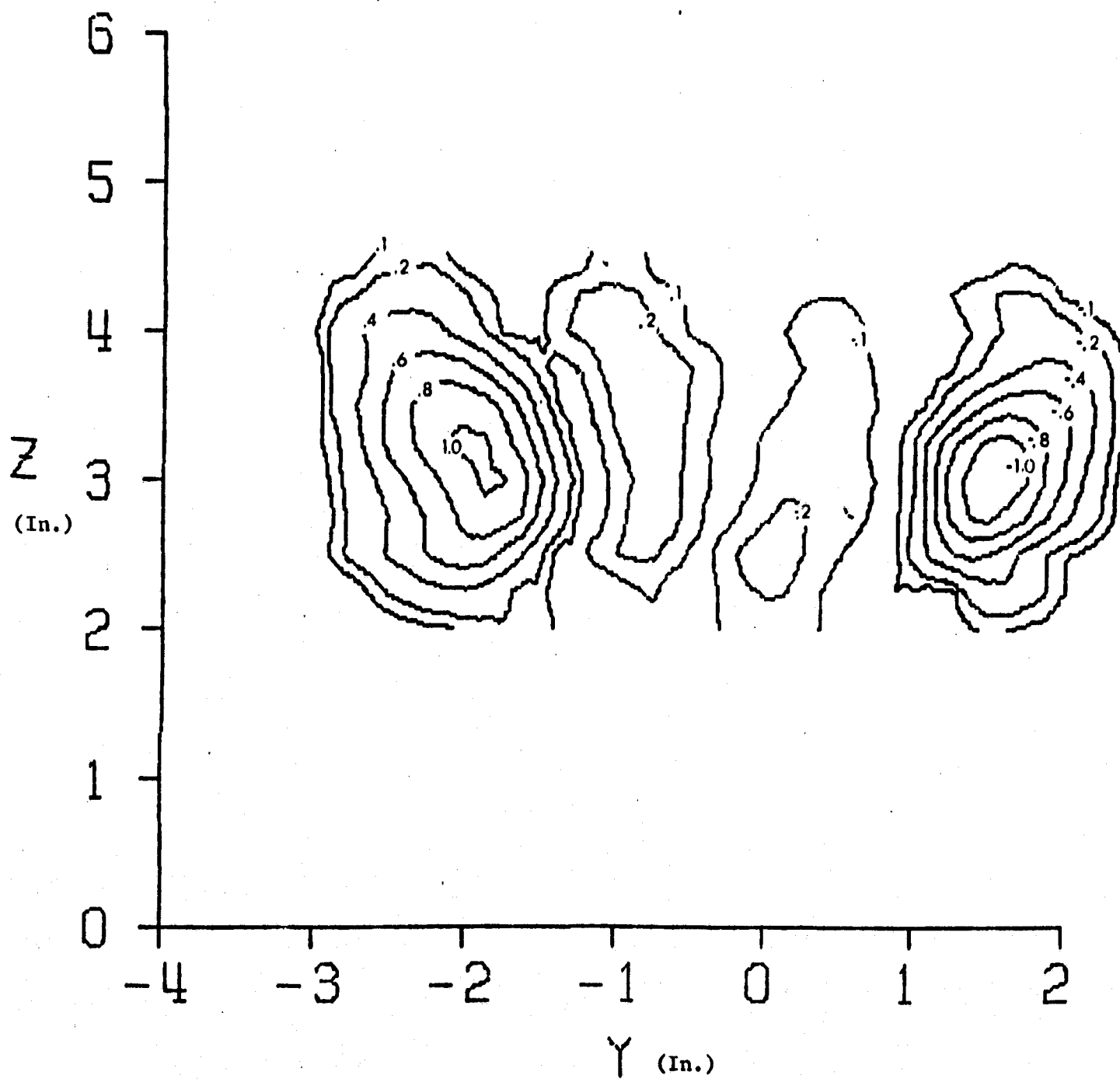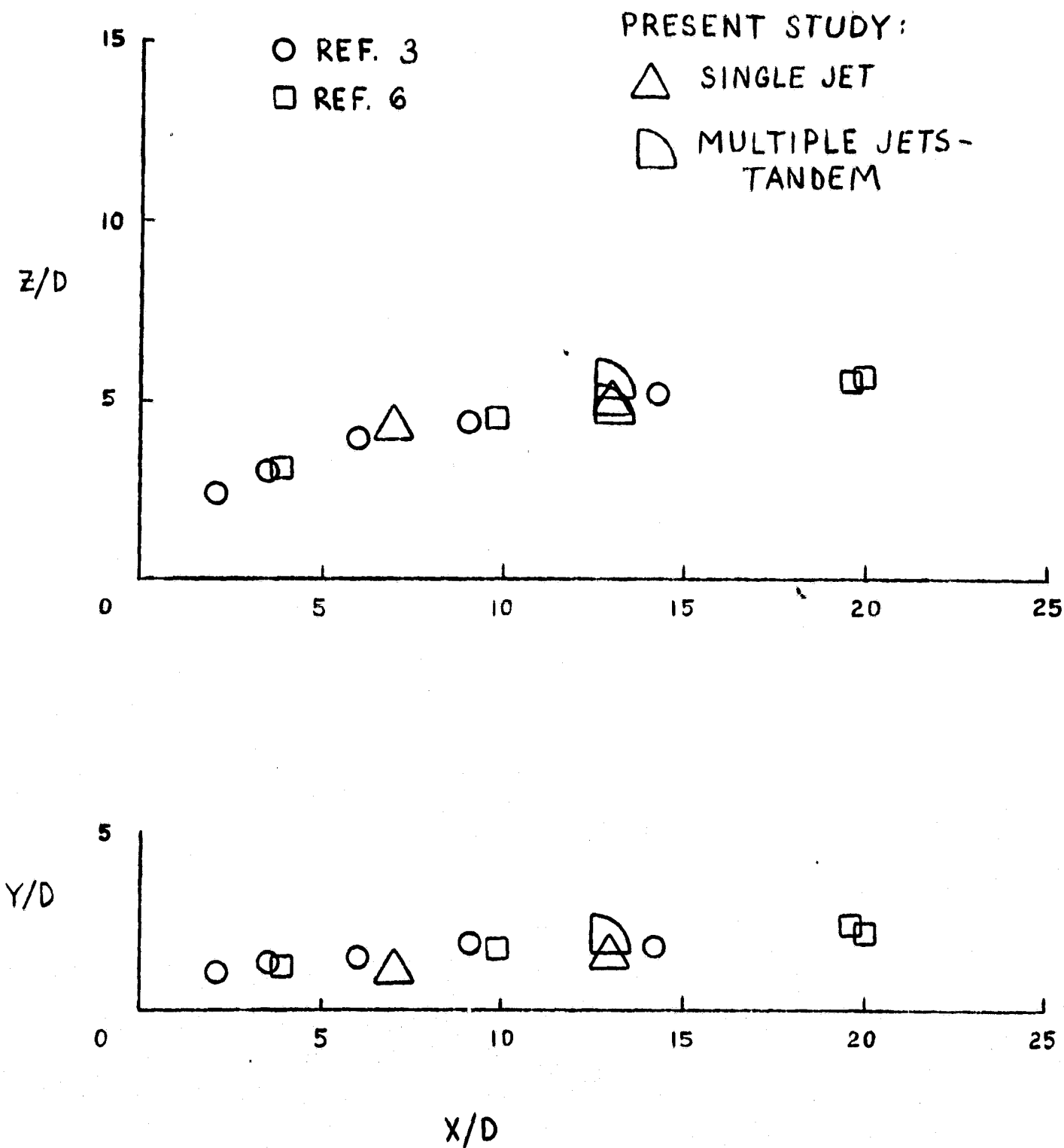
R=8.   X/D=8.66.

(c) Both jets.
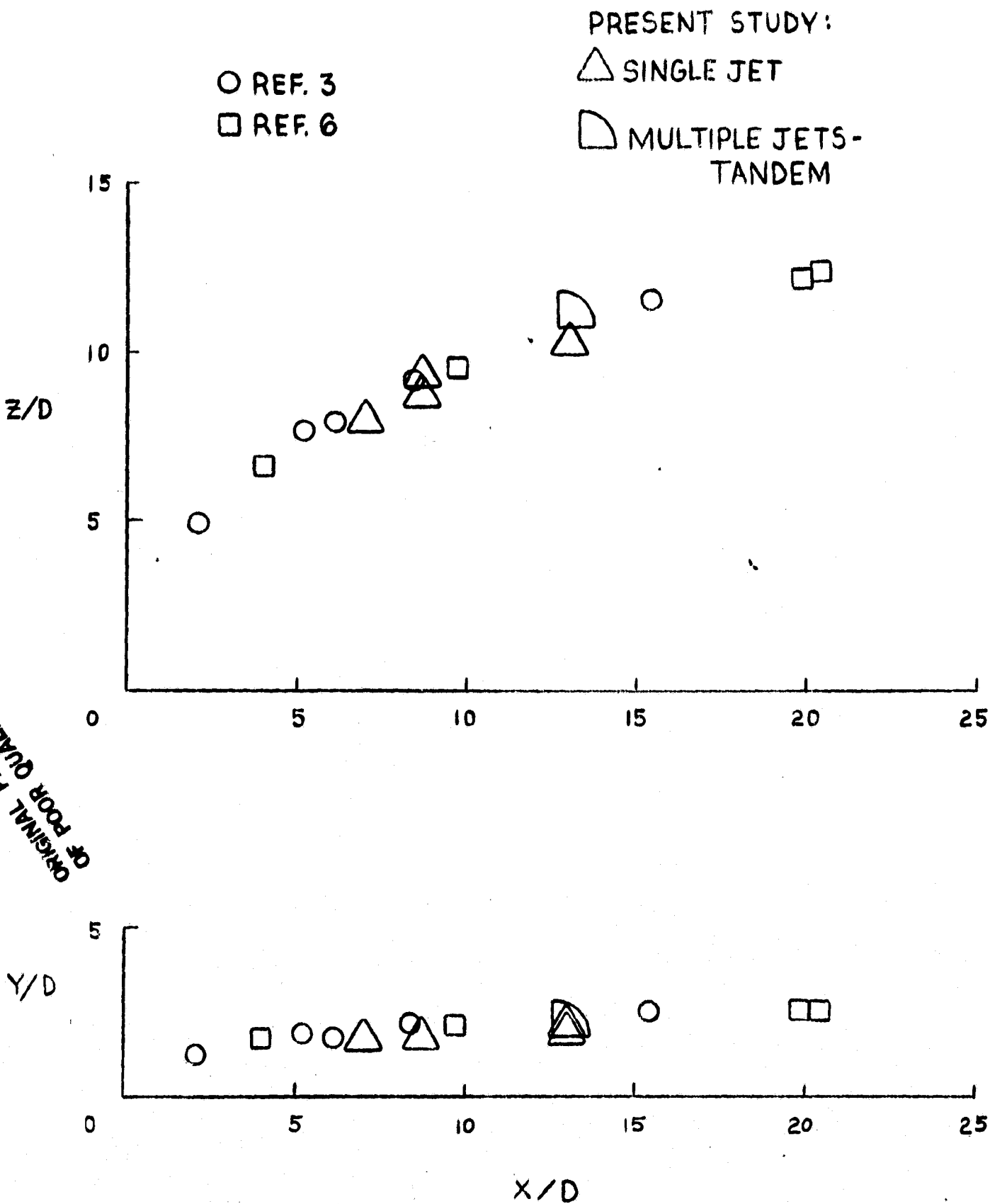Figure 12.   Continued.

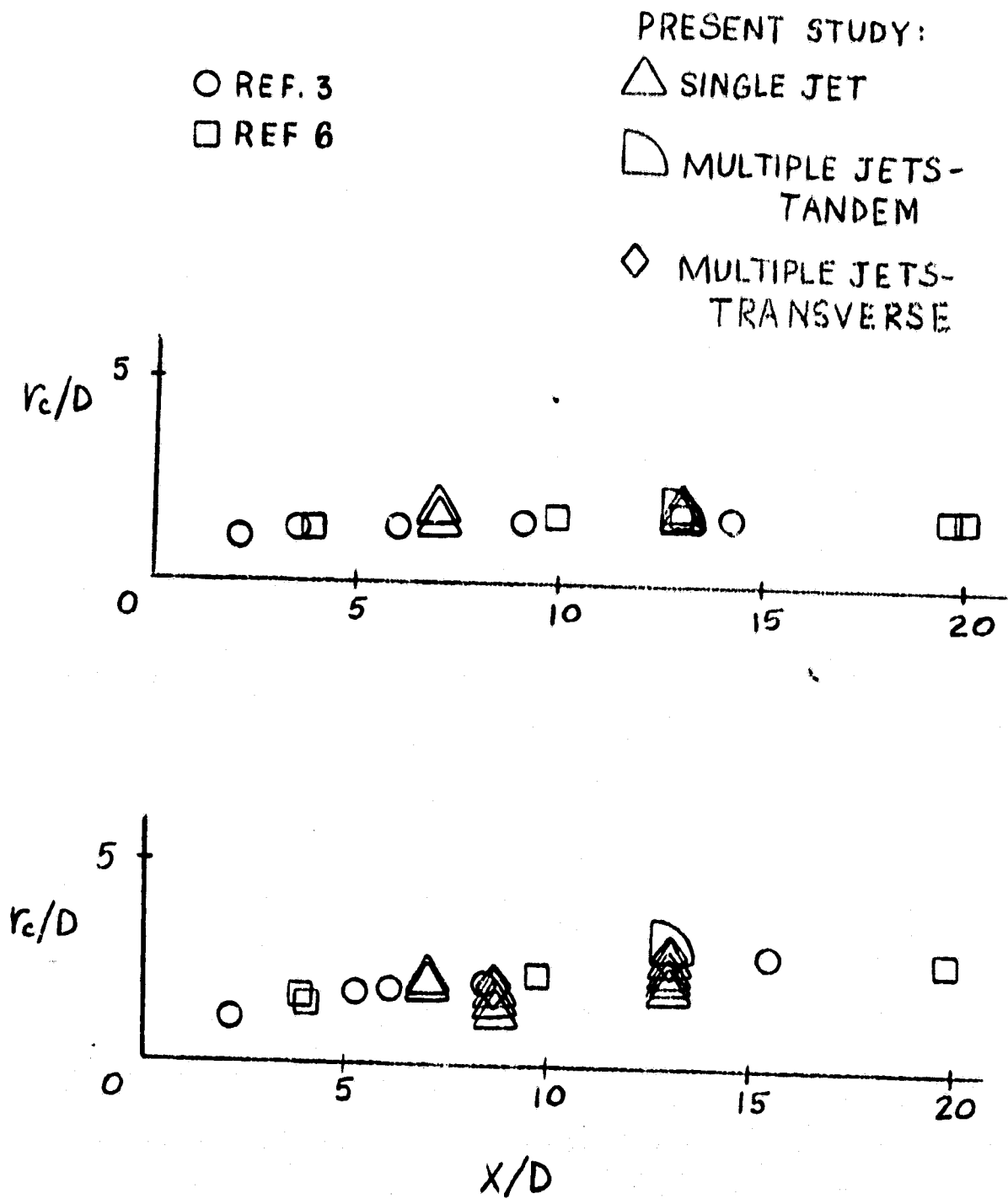Figure 13. Vortex geometry, R=4.

Figure 14. Vortex geometry, R·8.

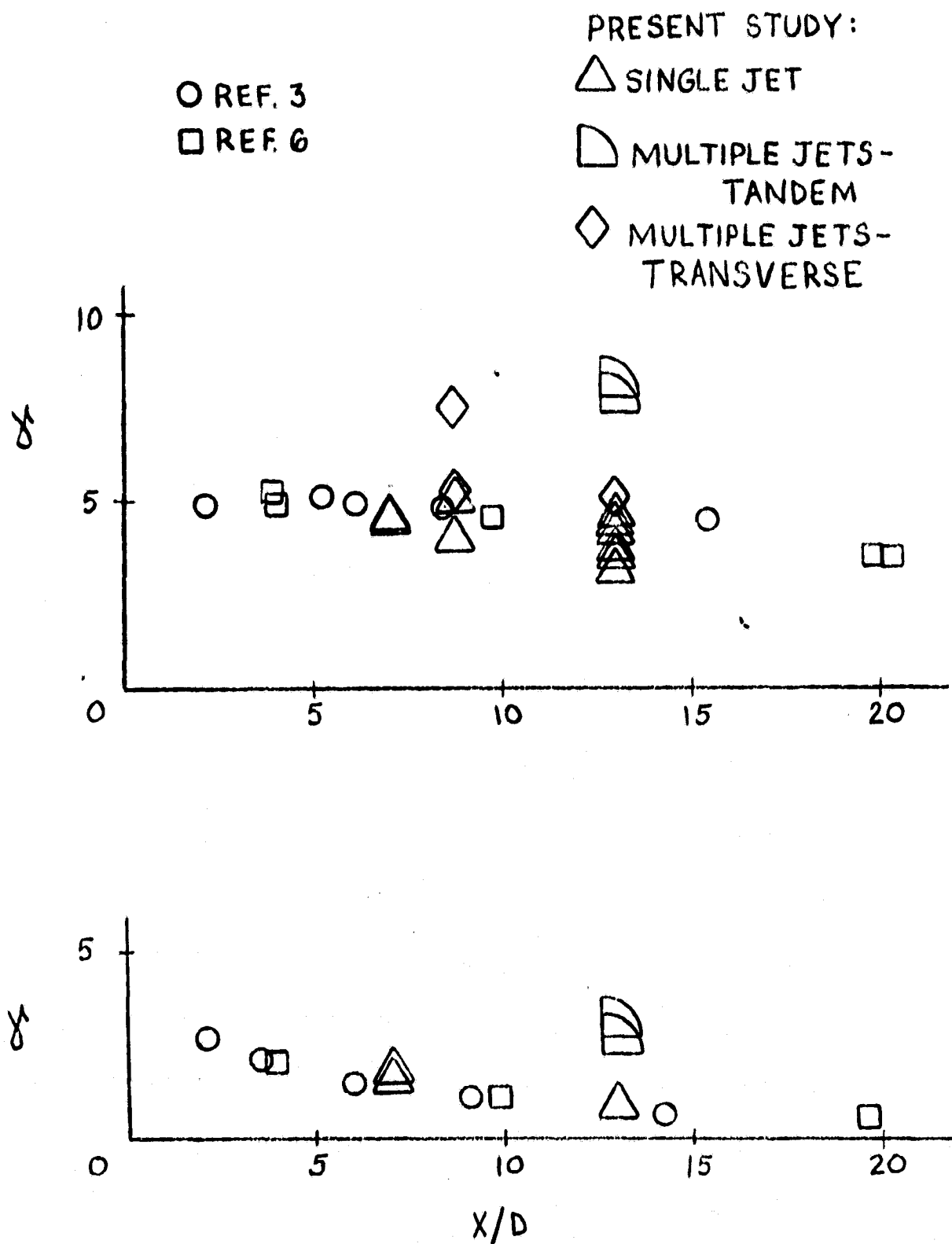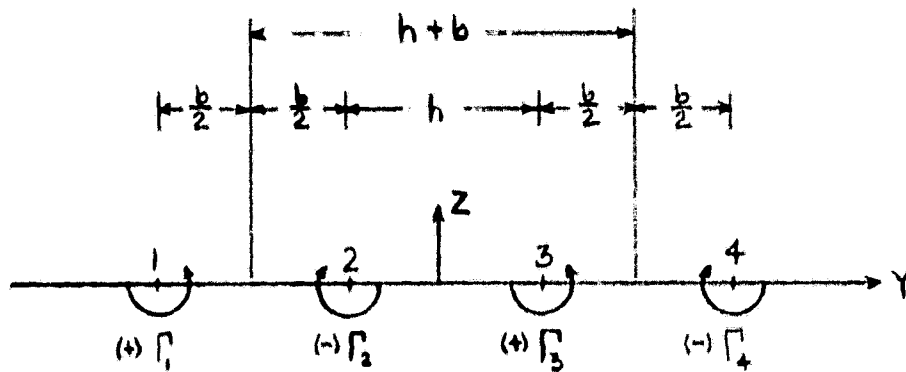Figure 15. Vortex core. R=4, upper. R=8, lower.

Figure 16. Vortex strength. R=4, lower, R=8, upper.

Velocity potential: $\phi = \frac{\Gamma\theta}{2\pi}$, where θ is measured for a vortex centered coordinate system.

For the above system, the velocity induced at 1 by 2, 3, 4:

$$\vec{V}_1 = \left[\frac{\Gamma_2}{2\pi b} - \frac{\Gamma_3}{2\pi(b+h)} + \frac{\Gamma_4}{2\pi(2b+h)} \right] \hat{k}$$

where $\hat{k}$ is the unit vector in the z direction.

The velocity induced at 2 by 1, 3, 4:

$$\vec{V}_2 = \left[\frac{\Gamma_1}{2\pi b} - \frac{\Gamma_3}{2\pi h} + \frac{\Gamma_4}{2\pi(b+h)} \right] \hat{k}$$

For the simple case of $b = h$, $|\Gamma_1| = |\Gamma_2| = |\Gamma_3| = |\Gamma_4|$

$$\vec{V}_1 = \frac{5}{6} \left(\frac{\Gamma}{2\pi b} \right) \hat{k} \quad \text{and} \quad V_2 = \frac{1}{2} \left(\frac{\Gamma}{2\pi b} \right) \hat{k}$$

$$\frac{V_1}{V_2} = 1.67$$

If $b > h$, $\frac{V_1}{V_2}$ increases.

Figure 17. Potential flow calculations.